22 P.

X-615-64-109

TM X-55004

RESULTS FROM THE IMP-I RETARDING POTENTIAL ANALYZER

BY
G. P. SERBU

MAY 1964

NASA

GODDARD SPACE FLIGHT CENTER

GREENBELT, MARYLAND

RESULTS FROM THE IMP-I RETARDING POTENTIAL ANALYZER

by

G. P. Serbu
NASA-Goddard Space Flight Center
Greenbelt, Maryland, USA

23929

ABSTRACT

Presented are some preliminary experimental results obtained with a planar geometry retarding potential analyzer which was flown on the IMP-I Satellite. The plasma energy spectrum for both ions and electrons was measured in the range from 0 to 100 electron volts. Charged particle density measurements have been obtained continuously from 1000 km to 30 earth radii.

The results show a sharp decrease of about an order of magnitude in charged particle density at about 4.5 R_E, similar to the decrease deduced from whistler observations. The electrons exhibited thermal energies for geocentric distances less than 4.5 R_E. The average electron energy then increased gradually to values above 100 electron volts at about 8 R_E. The observed satellite potential was less than 1 volt positive. author

INTRODUCTION

Measurement of the ionized plasma enveloping the earth have been reported on by numerous investigators to date. The region to 30 earth radii has been extensively traversed by a number of satellites, beyond this distance measurements have been made from the Soviet Lunik probes and the American Mariner series.

Primarily the energy spectrum of positively charged particles, presumably protons, has been investigated, and only a few measurements on the electron spectrum below 10 keV are available to date.

Presented are some preliminary experimental results obtained with a retarding potential experiment designed to measure the number density and the energy of ions and electrons in the energy range below 100 eV at distances to 30 earth radii.

2. INSTRUMENTATION

The retarding potential analyzer gives information on the arrival direction and energy distribution of both ions and electrons up to 100 eV. The detector is a charged particle trap of planar geometry which is programmed with appropriate voltages such that the number of charged particles of either polarity can be measured separately as a function of a given energy interval.

The charged particle trap is a circular cup 7 cm in diameter mounted such that the aperture is flush with the satellite skin, and so that it looked out at right angles to the spin axis of the satellite.

The outside aperture is a hole of 5 cm^2 in area over which is stretched a fine wire mesh of 95% transmission to light. Surrounding the aperture is a tungsten surface of 35 cm^2 area which is electrically connected to the aperture grid. Spaced

parallel to the aperture and 4 mm behind it is the retarding grid. The collector is a disk of tungsten which is, parallel to, and 4 mm behind the retarding grid. The geometry and size of the aperture and the relative spacings provide a view angle for the trap of 5 steradians. Figure 1 shows the total viewing direction of the trap as it was spin-modulated at the satellite spin rate of 22 revolutions per minute. Nearly all directions are viewed during one revolution, with the sun vector lying within 20^{o} of the normal to the trap once each revolution.

The collector current is measured by a logarithmic amplifier whose analog output is presented directly to telemetry. The electrometer sensitivity is from 10^{-11} to 10^{-6} amperes of either polarity. An internal current calibrator is used to check the electronics in flight.

Figure 2 shows a schematic diagram of the sensor and also the sequence of voltages programmed to the various trap elements in order to define the four modes of operation: low (30 eV) and high (100 eV) ion spectrum and the low (30 eV) and high (100 eV) electron spectrum. A mechanical programmer which operates in synchronism with the telemetry system, is used to switch the voltages to the trap. As an example, the low energy (30 eV) ion spectrum is done as follows: the aperture grid and guard electrode are maintained at -30 volts with respect to the satellite skin, thus all electrons with energy less than 30 eV are excluded from the trap and all positive ions are accelerated through the aperture. The retarding grid voltage is changed in fifteen equal steps between zero volts and plus 28 volts. A current measurement is made and telemetered at each retarding potential step. Only those ions with energies in excess of the retarding potential will pass through the retarding grid and impinge on the collector. In this manner a current voltage characteristic is obtained for ions with energy below 30 eV.

During the ion measurement photoemission current from the collector appear as a positive current with an expected magnitude of about 10^{-8} amperes. As the collector views the sun the photoemission current amplitude will vary as the cosine of the angle between the sun vector and the trap normal and it will be repetitive with the spin cycle, thus the photocurrent can be corrected for in the data. A highly accurate solar aspect sensor is used to find the precise time that the sun vector lies in the plane normal to the trap.

The electron mode of operation is such that the positive 20-volt potential on the collector suppresses all photoelectron emission from the collector. However, photoelectrons can be emitted from the grids and will appear as a negative current, the expected value being 5.10^{-10} amperes. Grid photoemission currents can also be easily corrected for in the electron data.

The 30 eV and 100 eV ion spectra are obtained first and then the trap voltages are reversed and the 30 eV and 100 eV electron spectra are obtained. The entire ion and electron sequence is repeated once every 10 minutes, each individual 15 step spectrum analysis is done within 5.4 seconds.

3. RESULTS

Figure 3 shows a 30 eV electron spectrum which was obtained at 2.2 earth radii (R_e) geocentric distance. The data points are the measured current values, plotted on a logarithmic scale as a function of the known retarding potential voltage. The resultant semilogarithmic plot is a current-voltage characteristic which yields information on the mean energy and the density of electrons. The observed two orders of magnitude decrease in collector current with two volts negative retardation suggests a maxwellian distribution of electron velocities. A second component or high-energy "tail" to the distribution is noted beyond 2 volts. The primary slope yields a value of

0.3 eV or an equivalent electron temperature of 3500°K. From the governing equation:

$$I_- = \tfrac{1}{4} N_e \bar{V}_- eA\, e^{-ve/kT_e} \qquad (1)$$

where I_- is the measured current, N_e the electron density, $\bar{V}_-$ most probable velocity, A area, v retarding potential, e electronic charge, k Boltzmann constant and T_e the electron temperature. We compute the electron density if A, the effective area is known. Low energy electrons which normally would not impinge on the aperture are deflected into the aperture along the accelerating +30 volt electric field lines; thus a uncertainty in the effective collection area exists. Using the geometric aperture area we compute a flux of 5×10^{10} electrons/cm^2sec, this flux could be a factor of 10 too large due to the collection area uncertainty. Using equation (1) a flux of 5.10^{10} el/cm^2sec with a mean energy of 0.3 eV at 2.2 R_e; if maxwellian in distribution, represents a electron density of 3.5×10^3 el/cm^3. The high energy component of 5.0 eV has an upper flux value of 3.10^8 el/cm^2sec. It has been suggested by Hanson (1) that at 7000 km, approximately this altitude, a 10^8 el/cm^2sec flux of 5 eV photoelectrons exists. These photoelectrons are formed at altitudes above 300 km and diffuse along magnetic field lines; Mariani (2) extended the work of Hanson and describes the role that these photoelectrons may play in the explanation of the "equatorial" or "geomagnetic" anomaly. Since these electrons are constrained to follow field lines the flux will drop off with the cube of the distance; thus beyond 3 R_e this flux should be below the minimum sensitivity of this experiment.

In Figure 3 the current to the trap decreases below the minimum sensitivity at retarding potentials greater than -12 volts, thus fewer than 1×10^7 electrons/cm^2sec exist with

energy in excess of 12 eV. The two photoemission peaks correlate well with the indicated sun position. The magnitude of the photoemission current is consistent with the value of 5×10^{-10} amperes computed on the basis of solar illumination of the 95% transparent grid.

Satellites, in general, are charged negative; Jastrow and Pearse (3), Beard and Johnson (4), owing to the high velocity of electrons compared with either the velocity of the satellite or the thermal velocity of ambient ions. However, at very high altitudes, and in interplanetary space, where the electron concentrations are small, a satellite might tend to have a net positive charge due to the photoelectric effect (Ja L Al'Pert et al, 5).

A direct measurement of the net charge, or the resultant potential difference between satellite and plasma as a consequence of the accumulated charge, can be based on observed current-voltage characteristics, Loeb (6); such as the one in Figure 3. Since a positive potential will accelerate ambient electrons to the satellite the measured electron current will not be retarded until an opposing voltage of equal magnitude to that of the satellite potential is reached. At that potential the characteristic will change slope and a further increase in negative voltage will retard the electron current. It is evident from the data of Figure 3 that a break in the curve could exist for potentials more negative than +2 volts; therefore, the satellite potential is not more than 1 volt positive, more probably it is only a few tenths of a volt negative. There is not evidence throughout the magnetosphere that the satellite potential is ever positive.

The 30 eV electron spectrum obtained at 4.6 R_e geocentric, is shown in Figure 4. The slope of this characteristic yields a electron energy value of 1.4 eV, or an equivalent gas

temperature of 16,400°K. A maximum flux of 9×10^9 electrons/cm^{2}sec is computed from the data, assuming the effective area to be equal to the geometric area. Converting to energy, Figure 4 data yields, 2.2×10^{-2} ergs/cm^{2}sec, thus when we compare this to the value of 1 to 10ergs/cm^{2}sec for particles with E≥200 eV obtained by the Explorer XII Cadmium Sulphide Total Energy Detector (CSDTE) Freeman et al (7), it is apparent that a large number of low energy electrons, E≤1.4 eV, exist in the second radiation belt, however, their energy content represents only a small fraction of the total particle energy Gringauz et al (8) infers from the Soviet charge particle traps that in this region an electron flux of 10^9 electrons/cm^{2}sec with energies below 200 eV is present.

Figure 5 shows a consecutive series of 30 eV electron spectra obtained between 7.2 and 8.3 R_e. It is apparent from all spectra that a residual negative current component is measured even at the maximum retardation voltage of 28 volts. Similar data, obtained at 9.2 R_e, is shown in more detail in Figure 6. The residual current amplitude is not roll modulated, thus at 8.2 R_e, on the sunlit side of earth, the satellite crossed into a region of omnidirectional electrons with energy in excess of 100 eV at a flux value of 1.5×10^8 electrons/cm^{2}sec. Gringauz et al (9,10,11) observed, with Lunik 1 and also with Lunik 2 and Mars 1, a flux of ($1\text{-}2 \times 10^8$ el/cm^{2}sec) at these distances with an energy larger than 200 eV, this region has been labeled by him as "the outermost belt of charged particles".

Figure 7 shows the 100 eV ion and electron spectra obtained at 9.0 and 9.1 R_e. The omnidirectional current residual in both traps at 100 volt retardation indicates that both ions and electrons are present in the outermost belt of charged particles with energies in excess of 100 eV. The data of Figure 7 may also be used to illustrate that the net current flow to the

satellite is essentially zero. At zero retardation, the current flow to the collector should be representative of any given area on the surface of the satellite, thus in order to maintain a constant satellite to plasma potential it must be shown that the net current flow to the satellite is zero. The photoemission current constitutes a positive current flow, i.e. electrons flowing outward from the satellite, which acts over the illuminated cross sectional area of the satellite. The negative current, is on the other hand, effective over the entire area of the satellite, since the ambient electron velocity exceeds the satellite velocity, and so electrons diffuse inward from all directions. In order to have a net zero current flow the ratio of the photocurrent to electron current must be equal to 4 which is the inverse ratio of the areas to which these current flows are effective. From Figure 7 the current ratios at zero volt retardation are seen to be 4; thus the trap currents at zero retardation are inferred to be representative of the overall current flow to the satellite and we deduce that the equilibrium satellite potential in sunlight is stabilized near zero volts.

The data in Figure 8 is representative of the trap currents at distances beyond 16.2 R_e geocentric. Positive and negative currents have been plotted as a function of orientation relative to the sun, this presentation was chosen since attempts at plotting the currents as a function of retarding voltages were fruitless. After subtracting out data points which are due to photoemission, the dashed curve; a residual net current in both traps is evident at 90 degree clockwise rotation from the sun, in the anti-solar direction the currents to the trap drop below 1×10^{-11} amperes. Since the retarding potentials do not effect the trap currents it is evident that the negative current measurement represents a net negative charge entering the trap

with energies in excess of 100 eV, and that the positive current measurement represents a sum of net positive charge plus secondary electron emission. Assuming a secondary electron emission efficiency of 100% these observations are consistent with the computation that what is seen beyond 16.2 R_e, i.e. in the solar wind region is a net flux of both ions and electrons of the order of 10^8 particles/cm^2 sec with energies in excess of 100 eV.

4. CONCLUSIONS

An overall summary of these observations may be made with the use of Figure 9, which is a plot of the electron flux as a function of geocentric distance. The three plotted curves were computed from the negative current in the trap found in the 0 to -5 volt retardation interval, the -5 to -10 volt and the -100 volt interval.

The flux of electrons with energies $0 \leq E \leq 5$ eV shows a steep decrease with distance between 3 and 5 R_e. This type of electron drop-off is in agreement with whistler observations, Carpenter (12) refers to the decrease as the "equatorial knee" and points out that the equatorial knee moves further out; i.e. beyond 3 R_e, during magnetically quiet periods. Out to about 3 R_e we note that the flux in the energy interval $5 \leq E \leq 10$ eV is decreasing with distance. This energy interval contains the previously mentioned Hanson photoelectrons, evident in Figure 2. Furthermore the drop off in flux evident in Figure 9 lends credulity to our belief that in this region we observe a flux of trapped photoelectrons produced at altitudes above 300 km.

Beyond 3 R_e an increase in the flux of electrons with energy $5 \leq E \leq 10$ eV is noted, at 7 R_e this flux is comparable to the flux of lower energy electrons. The error bars in the figure reflect the previously discussed uncertainly in the "effective collection area". Thus the overall picture is one

of an initial sharp decrease in thermal electron concentration accompanied by an increase in the average energy of electrons, such that, at some 7 R_e geocentric there are nearly as many electrons with energy greater than 5 eV as there are those with energy below 5 eV. At 8.2 R_e geocentric, on the sunlit side of earth, with a payload-earth-sun angle of 25 degrees, a flux of 2×10^8 electrons/cm^2 sec omnidirectional electrons with energy greater than 100 eV is observed. There is no significant variation in this flux rate across the magnetosphere; the magnetosphere boundary was determined through the IMP-I magnetometer data of Ness (12). Beyond 16.2 R_e the flux of these omnidirectional particles drops off sharply. Whereas, crossing of the magnetosphere boundary is not evident from the trap data, the crossing of the shock front is. On the earth side of the shock front the trap currents are governed by the retarding potential voltages, outside the shock front the trap currents are governed by the trap-sun angle orientation.

The recent controversy Gringauz (13), Van Allen (14), concerning the observations of particles in the outermost belt of charged particles and whether or not these particles are trapped is not resolved on the basis of these IMP observations; since it is possible to explain the observed constant flux across the magnetosphere boundary either on the basis of some unknown mechanism for solar wind penetration as suggested by Gringauz or on the basis that the total trapped flux inside the boundary just equals the flux outside the boundary, a possibility not excluded by the measurements of Explorer XII and IV, Frank et al (15).

5. ACKNOWLEDGEMENTS

Messrs. W. J. Archer and J. Luce were responsible for the instrumentation associated with this experiment. Also acknowledged are the helpful discussions with Mr. R. E. Bourdeau.

6. REFERENCES

(1) Hanson, W. B.
"Electron Temperatures in the Upper Atmosphere", Space Research III Proceedings of the Third International Space Sciences Symposium, pp. 282 - 302, North-Holland Publishing Company, Amsterdam, 1963.

(2) Mariani, F.
"Pitch Angle Distribution of the Photoelectrons and Origin of the Geomagnetic Anomaly in the F2 Layer", J.G.R., Vol. 69, No. 3, Feb. 1, 1964.

(3) Jastrow, R., and Pearse, C. A.
"Atmospheric Drag on the Satellite", J.G.R., Vol. 62, No. 3, Sept., 1957.

(4) Beard, D. B. and Johnson, F. S.
"Charge and Magnetic Field Interaction with Satellites", J.G.R., Vol. 65, No. 1, Jan., 1960.

(5) Al'Pert, Ja. L., Gurevic, A. V. and Pitaevskij, L. P.
"Effects Due to an Artificial Satellite in Rapid Motion through the Ionosphere or the Interplanetary Medium", Space Science Reviews, Vol. 11, No. 5, Nov., 1963, pp. 680-748.

(6) Loeb, L. B.
"Basic Processes of Gaseous Electronics", University of California Press, Berkeley and Los Angeles, 1955, pp. 331-371.

(7) Freeman, J. W., Van Allen, J. A. and Cahill, L. J.
"Explorer XII Observations of Magnetospheric Boundary and the Associated Solar Plasma on Sept. 13, 1961. J.G.R., Vol. 68, No. 8, April, 1963.

(8) Gringauz, K. I., Balandina, S. M., Bordovskii, G. A. and Shyutte, N. M.
"On the Results of Tests with Three-Electrode Charged Particle Traps in the Second Radiation Belt and in the Outermost Belt of Charged Particles", Planetary Space Science, 1964, Vol. 12, pp. 175-179. Pergamon Press Ltd., Printed in Northern Ireland.

(9) Gringauz, K. I., Bezrukirkh, V. V., Ozerov, V. D. and Rybchinskii, R. E.
"A Study of Interplanetary Ionized Gas, Energetic Electrons and Solar Corpuscular Radiation Using Three-Electrode Charged Particle Traps on the Second Soviet Cosmic Rocket", DOKL. AKAD NAUK SSSR 131, 1301 (1960).

(10) Gringauz, K. I., Kurt, V. G., Moroz, V. I. and Shklovskii, I. S.
"Ionized Gas and Fast Electrons in the Neighborhood of the Earth and in Interplanetary Space" [ISKUSSTVENNYE SPUTNIKI ZEMLI (Artificial Satellites of the Earth)] No. 6, p. 108, IZD, AKAD. NAUK. SSSR, Moscow, 1961.

(11) Gringauz, K. I., Bezrukikh, V. V., Musatov, L. S., Rubchinskii, R. E. and Sheronova, S. M.
"Measurements Made in the Earth's Magnetosphere by Means of Charged Particle Traps Aboard the Mars 1 Probe", Space Research Proc. Intern. Space Science Symp. 4th Warsaw, 1963. North-Holland Publishing Company, Amsterdam, June, 1963.

(12). Ness, N. F.
(Private Communication)

(13) Gringauz, K. I.
"Remarks on Papers by J. W. Freeman, J. A. Van Allen and L. J. Cahill, Explorer 12 Observations of the Magnetosphere Boundary and the Associated Solar Plasma on September 13, 1961, and by L. A. Frank, J. A. Van Allen and E. Macagno, 'Charged-Particle Observations in the Earth's Outer Magnetosphere", J.G.R. Vol. 69, No. 5, March 1, 1964.

(14) Van Allen, J. A.
"Remarks on Accompanying Letter by K. I. Gringauz", J.G.R., Vol. 69, No. 5, March 1, 1964.

(15) Frank, L. A. Van Allen, J. A., and Macagno, E.
"Charged-Particle Observations in the Earth's Outer Magnetosphere", J.G.R., Vol. 68, No. 12, June 15, 1963.

FIGURE CAPTIONS

Figure 1 - Location and Viewing Sphere of the Retarding Potential Analyzer Aboard the IMP-I Satellite.

Figure 2 - Schematic Diagram of Sensor and the Various Programmed Voltages.

Figure 3 - The 30 eV Electron Spectrum for 2.2 R_e Geocentric.

Figure 4 - The 30 eV Electron Spectrum for 4.6 R_e Geocentric.

Figure 5 - A Successive Series of 30 eV Electron Spectra Depecting the Transit into a Region Characterized by a Residual Current in the Trap, Due to a Omnidirectional Flux of Electrons.

Figure 6 - The 30 eV Electron Spectrum for 9.2 R_e Geocentric.

Figure 7 - The 100 eV Ion and Electron Spectra Obtained at 9.0 R_e and 9.1 R_e Geocentric.

Figure 8 - The Ion and Electron Currents Plotted as a Function of Trap-Sun Angle Orientation. These Responses Typify the Data Obtained at Distances Beyond 16.2 R_e Geocentric on the first IMP-I Orbit.

Figure 9 - Plot of the Electron Flux as a Function of Geocentric Distance. Three Electron Energy Intervals are Shown.

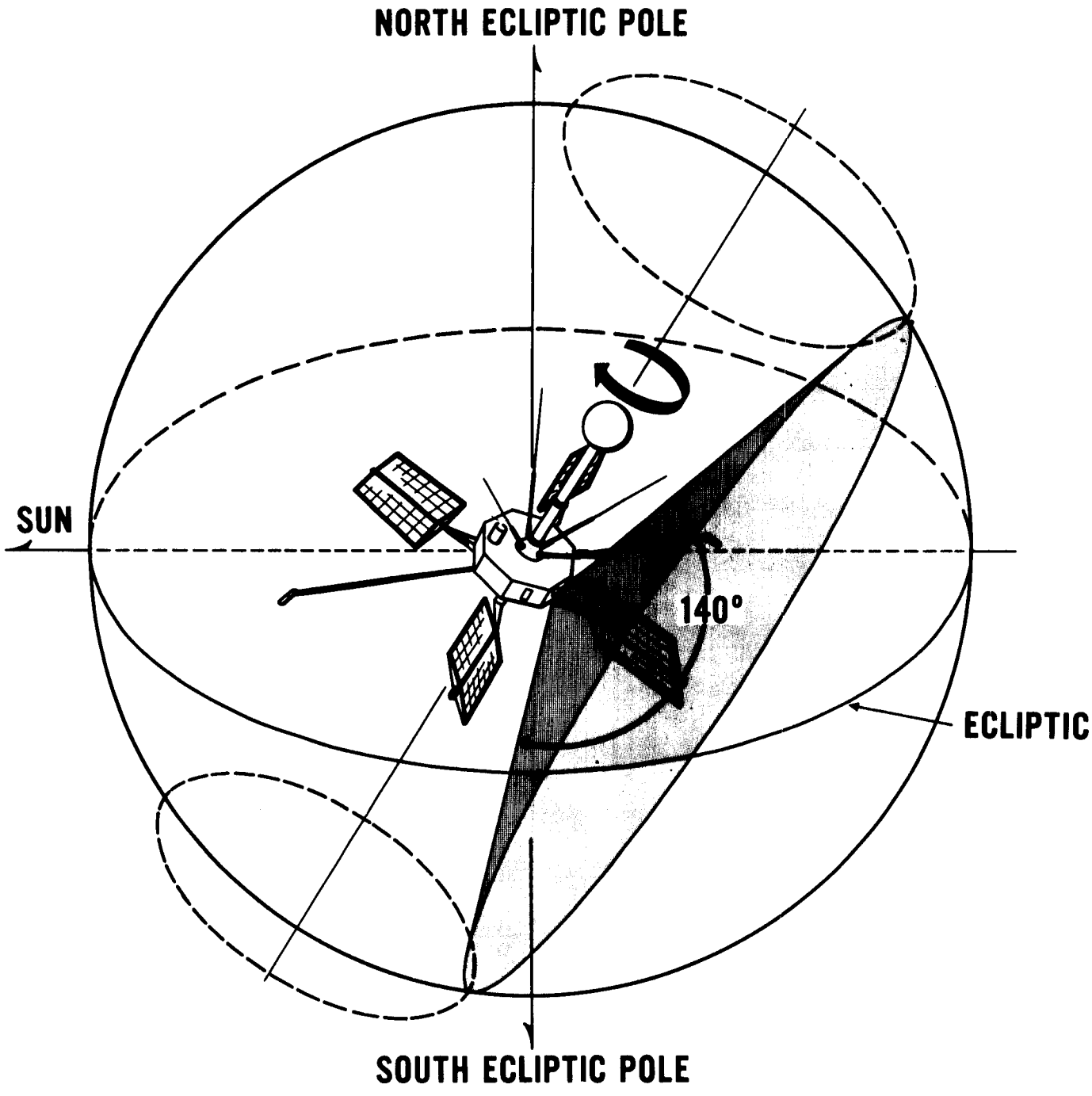
NORTH ECLIPTIC POLE
SUN
140°
ECLIPTIC
SOUTH ECLIPTIC POLE

IMP – A

RETARDING POTENTIAL ANALYSER

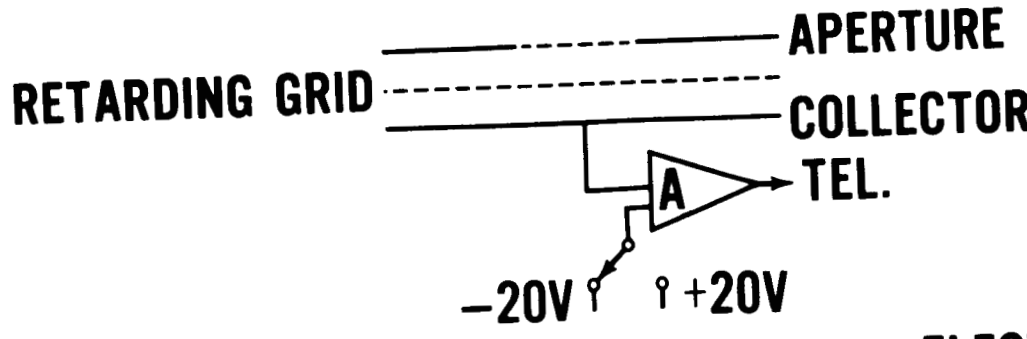

	ION		ELECTRON	
	LOW	HI	LOW	HI
APERTURE	–30V	–100	+30V	+100
RETARDING	0→+28V	0→+100V	0→–28V	0→–100V
COLLECTOR	–20V	–20V	+20V	+20V

APERTURE AREA=5cm^2

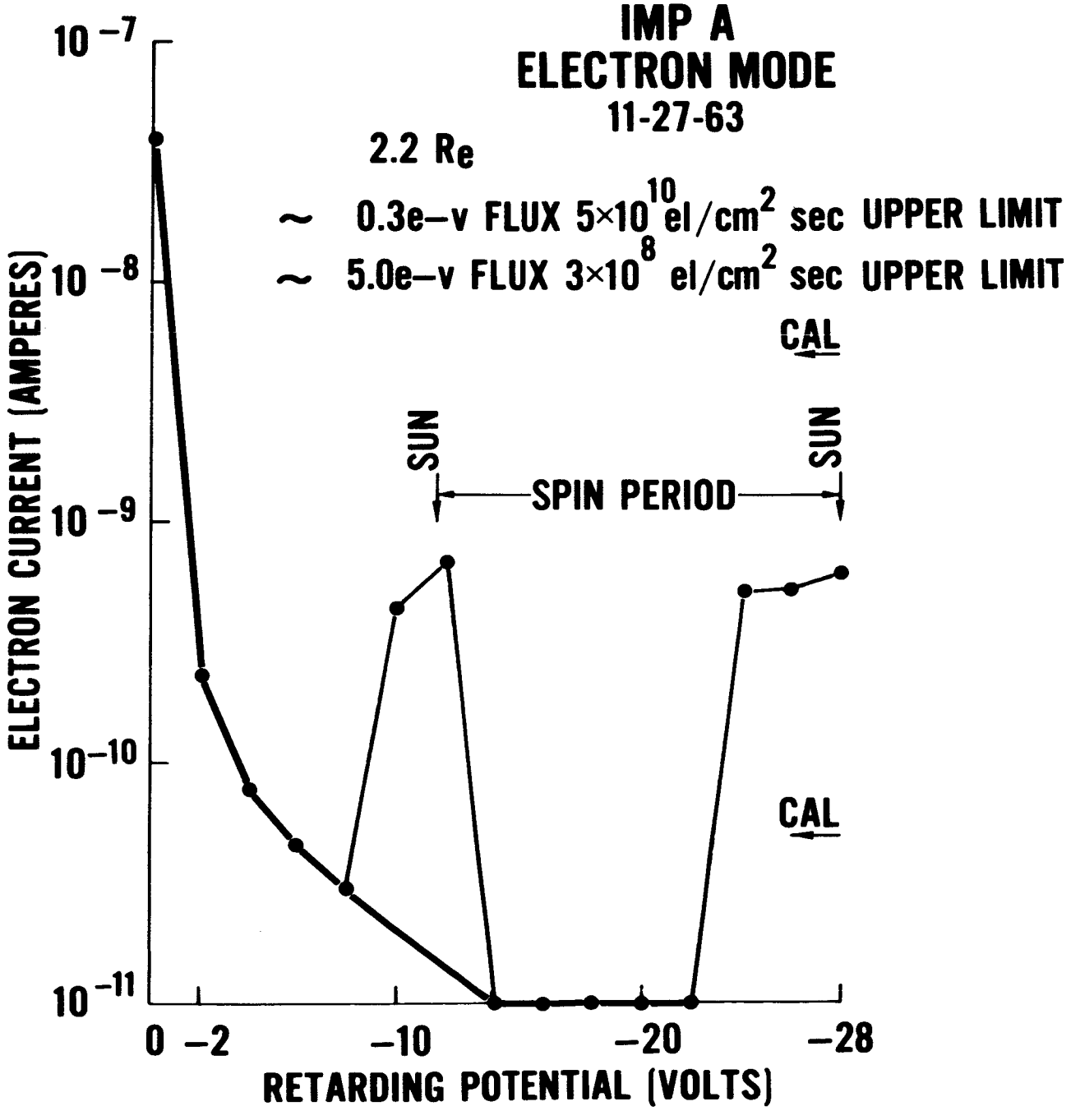
IMP A
ELECTRON MODE
11-27-63
2.2 Re
~ 0.3e–v FLUX 5×10^10 el/cm^2 sec UPPER LIMIT
~ 5.0e–v FLUX 3×10^8 el/cm^2 sec UPPER LIMIT
CAL
SUN
SUN
SPIN PERIOD
CAL
ELECTRON CURRENT (AMPERES)
10^-7
10^-8
10^-9
10^-10
10^-11
0
-2
-10
-20
-28
RETARDING POTENTIAL (VOLTS)

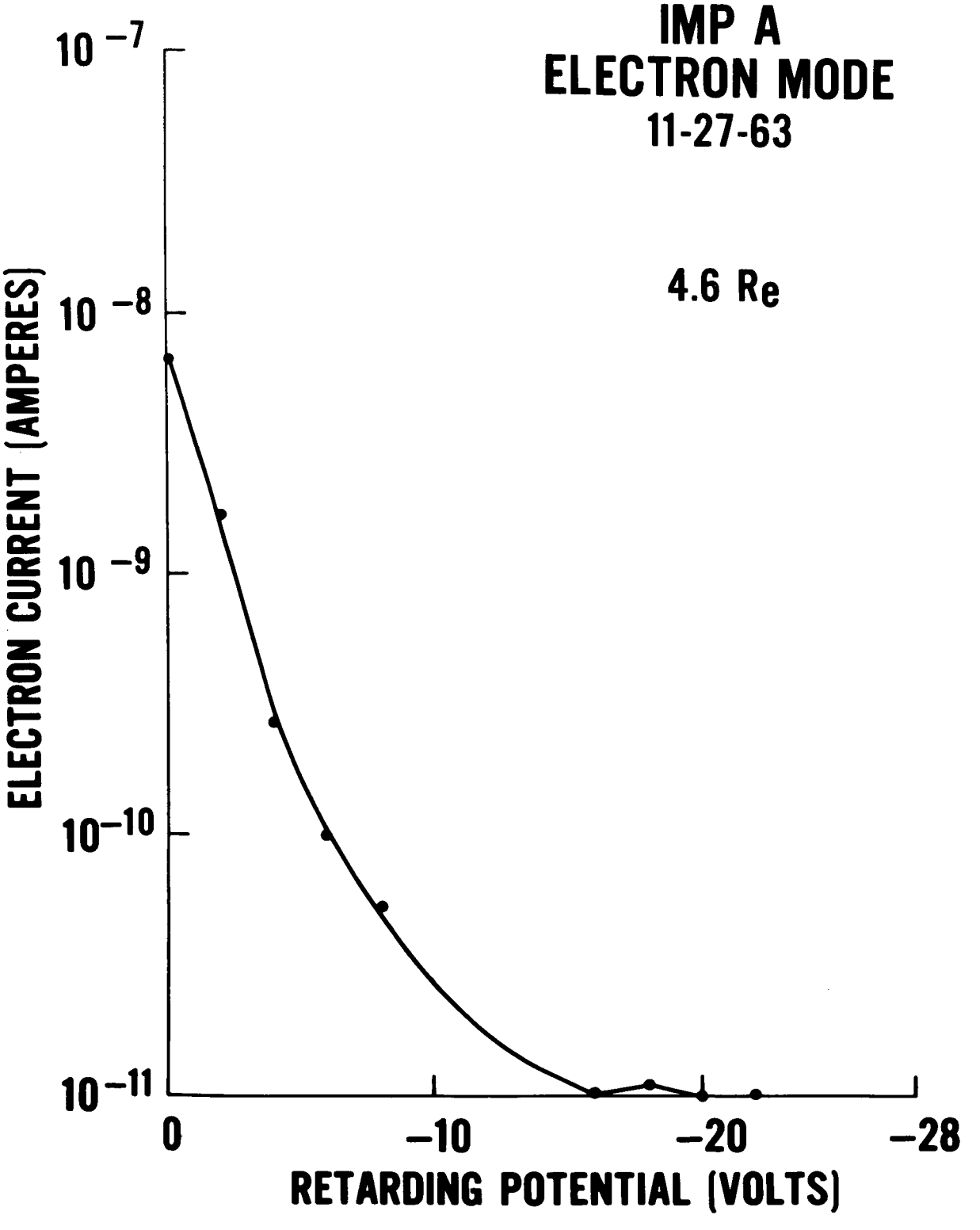
IMP A
ELECTRON MODE
11-27-63
4.6 Re
10 −7
10 −8
10 −9
10−10
10−11
ELECTRON CURRENT (AMPERES)
0
−10
−20
−28
RETARDING POTENTIAL (VOLTS)

IMP A

ELECTRON

MODE

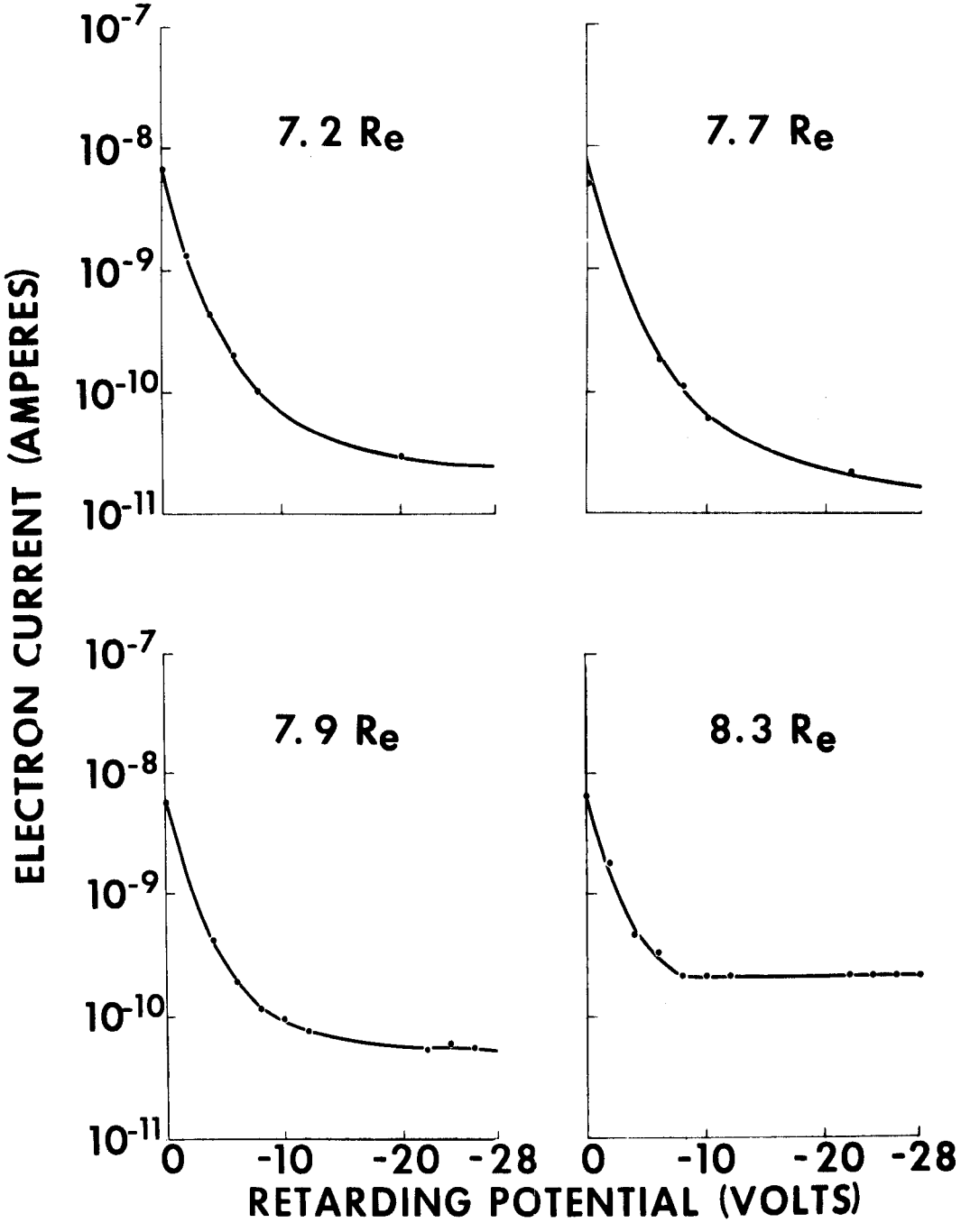

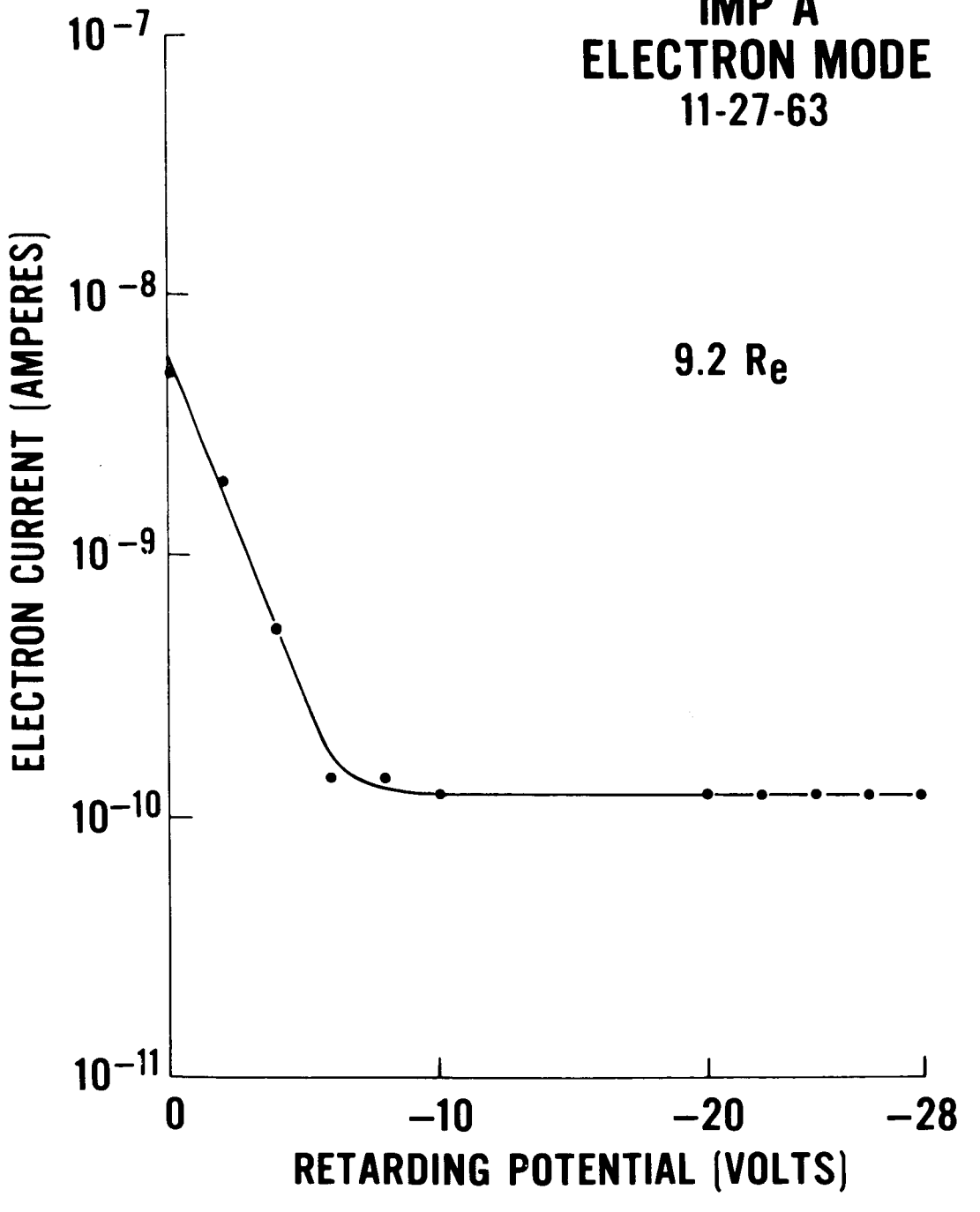
IMP A
ELECTRON MODE
11-27-63
9.2 Re
ELECTRON CURRENT (AMPERES)
10 -7
10 -8
10 -9
10-10
10-11
0
-10
-20
-28
RETARDING POTENTIAL (VOLTS)

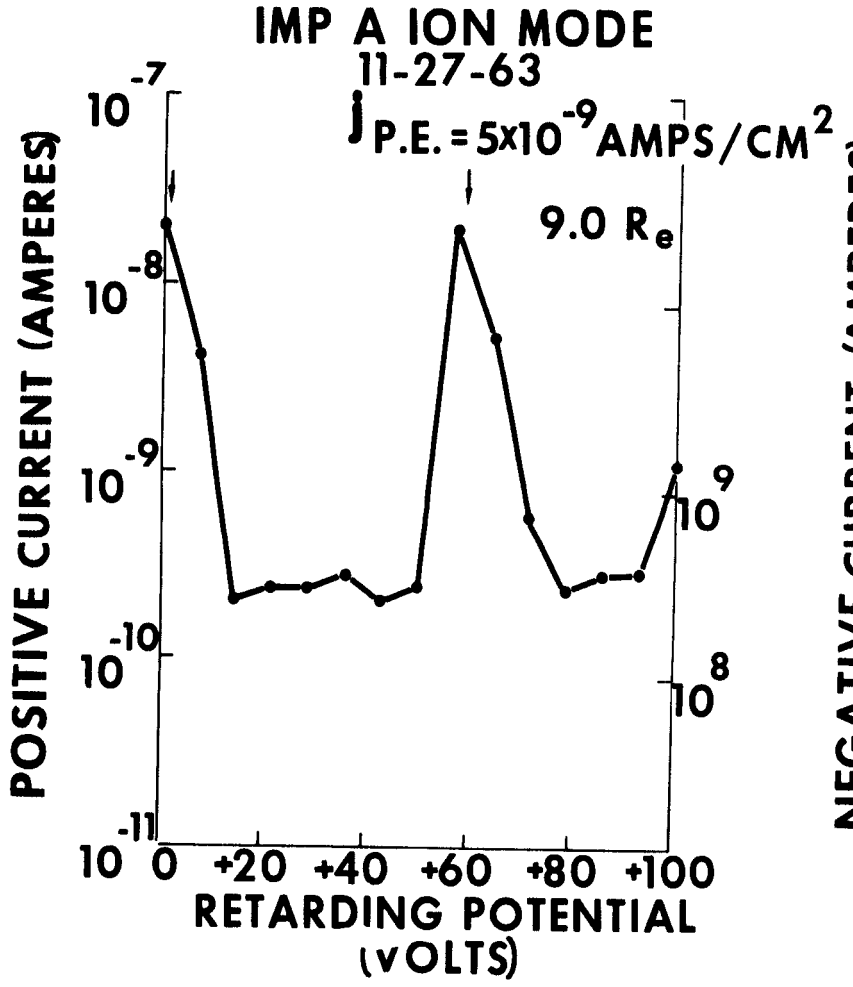
IMP A ION MODE
11-27-63
j P.E. = 5x10^-9 AMPS/CM^2
9.0 Re
POSITIVE CURRENT (AMPERES)
10^-7
10^-8
10^-9
10^-10
10^-11
10^9
10^8
0 +20 +40 +60 +80 +100
RETARDING POTENTIAL
(VOLTS)

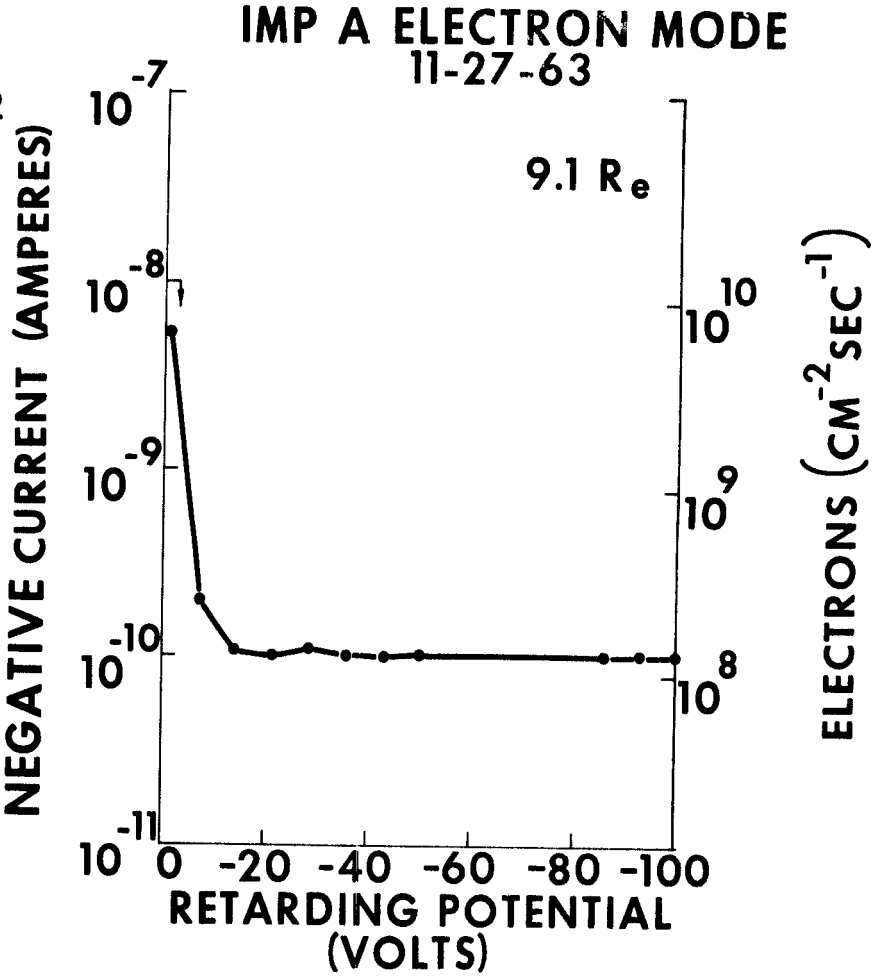
IMP A ELECTRON MODE
11-27-63
9.1 Re
NEGATIVE CURRENT (AMPERES)
10^-7
10^-8
10^-9
10^-10
10^-11
10^10
10^9
10^8
ELECTRONS (CM^-2 SEC^-1)
0 -20 -40 -60 -80 -100
RETARDING POTENTIAL
(VOLTS)

IMP A
11-27-63

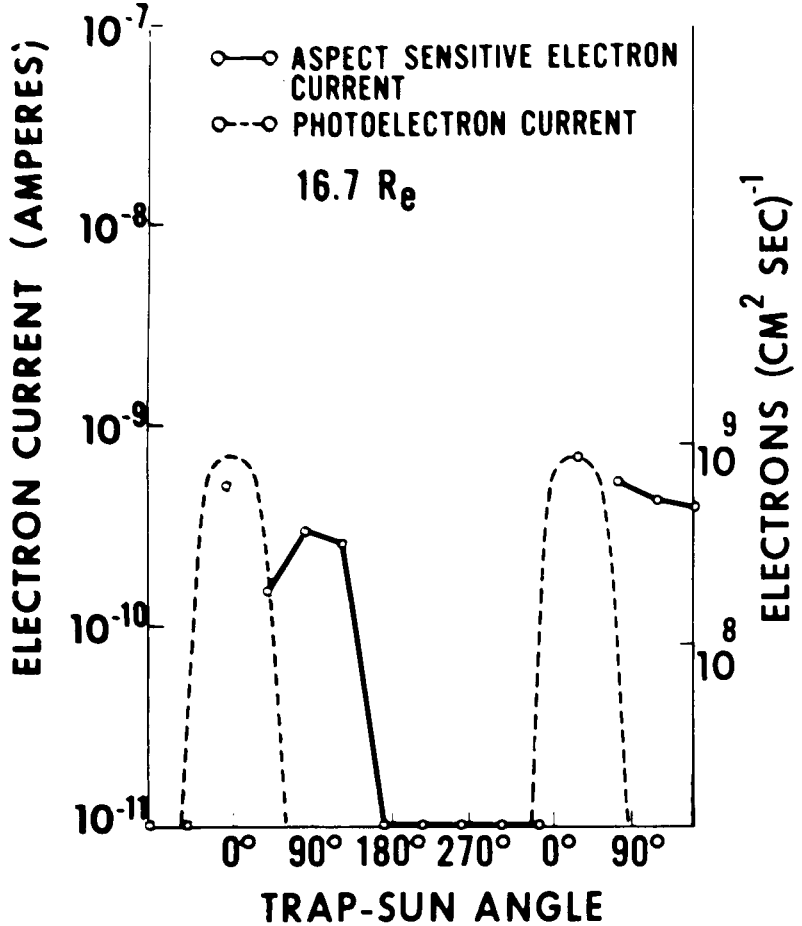
ASPECT SENSITIVE ELECTRON CURRENT
PHOTOELECTRON CURRENT
16.7 Re
ELECTRON CURRENT (AMPERES)
ELECTRONS (CM2 SEC)-1
10-7
10-8
10-9
10-10
10-11
10
9
10
8
0° 90° 180° 270° 0° 90°
TRAP-SUN ANGLE

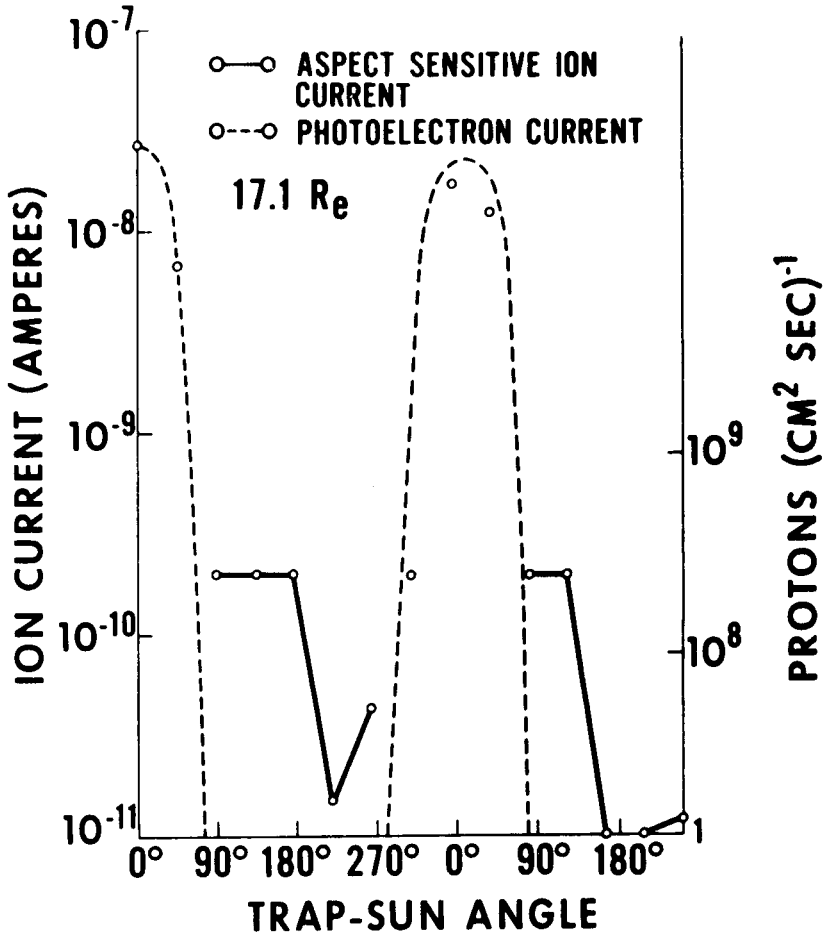
ASPECT SENSITIVE ION CURRENT
PHOTOELECTRON CURRENT
17.1 Re
ION CURRENT (AMPERES)
PROTONS (CM2 SEC)-1
10-7
10-8
10-9
10-10
10-11
10
9
10
8
1
0° 90° 180° 270° 0° 90° 180°
TRAP-SUN ANGLE

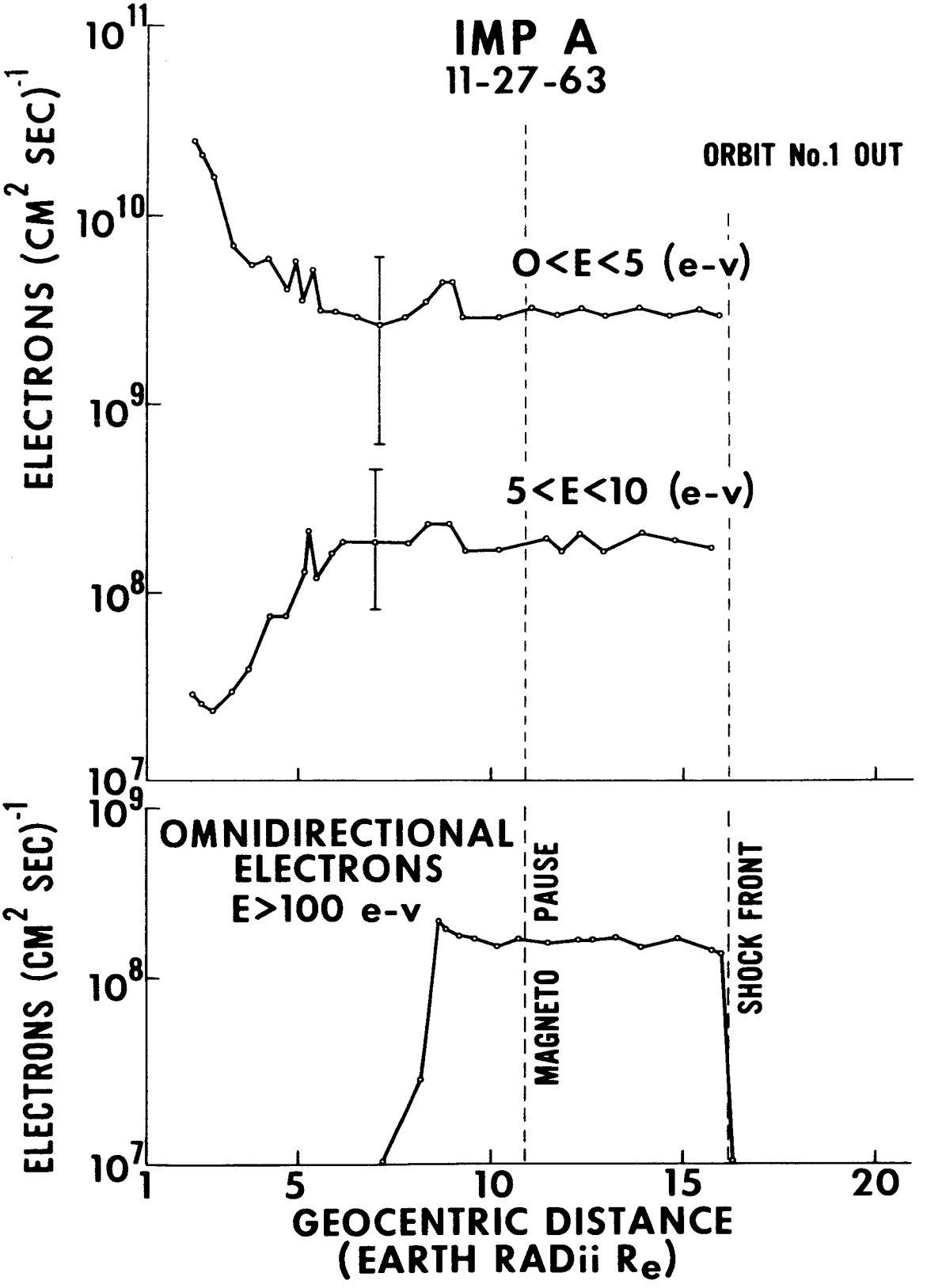
IMP A
11-27-63
ORBIT No.1 OUT
ELECTRONS (CM^2 SEC)$^{-1}$
10^{11}
10^{10}
10^9
10^8
10^7
O<E<5 (e-v)
5<E<10 (e-v)
OMNIDIRECTIONAL
ELECTRONS
E>100 e-v
MAGNETO PAUSE
SHOCK FRONT
1
5
10
15
20
GEOCENTRIC DISTANCE
(EARTH RADii R_e)